

## Dual-sensor data and enhanced depth imaging sheds new light onto the mature Viking Graben area

Marielle Ciotoli<sup>1</sup>, Sophie Beaumont<sup>1</sup>, Julien Oukili<sup>1</sup>, Øystein Korsmo<sup>1</sup>, Nicola O'Dowd<sup>1</sup>, Grunde Rønholt<sup>1\*</sup> and Volker Dirks<sup>1</sup> discuss how the combination of dual-sensor broadband data and advanced depth imaging technology is helping to reveal new hydrocarbon plays in the mature Viking Graben basin.

The Viking Graben area in the Central North Sea was the initial focus of a series of early 3D GeoStreamer dual-sensor surveys between 2009 and 2012 (Figure 1). These MultiClient surveys immediately demonstrated significant image quality improvements achieved with the dual-sensor towed streamer seismic in an area characterized by significant subsurface complexity.

After more than 50 years of active exploration, the Viking Graben is widely regarded as a mature basin whose

petroleum system is thought to be well understood. Many of the classic hydrocarbon targets of the region, including the large rotated Jurassic fault blocks of Gullfaks and Oseberg, and the Paleocene and Eocene fan systems of the Heimdal and Frigg fields, have already been exploited. Challenges remain to stratigraphic interpretation and mapping of sands within the Upper Jurassic and it is therefore important to have data which has sufficient penetration and accurate positioning of reflectors to continue to explore these levels. Determining the exploration opportunities beyond these classic targets also requires optimization of the seismic data.

The Eocene sands have been extensively mapped, but the Paleocene fans are less well known. Although the play is proven, the more subtle sands of the Ty and Maureen formations have been masked by artefacts caused by shallow events. In addition, several of the classic plays have now become the subject of re-evaluation. Better resolution and deeper signal penetration with dual-sensor data has provided detailed insight into many of these plays and also improved the understanding of the overall connectivity of several highly compartmentalized reservoirs that are often comprised of a variety of barriers and baffles.

In order to improve the understanding of the geology within this established area and to be able to exploit the fields to their full potential, modern seismic data need to be consistently re-evaluated and subjected to new processing techniques. The remobilized and injected reservoir sands of the Volund field were considered unique at the time of its discovery in 1994, however, many other recent discoveries are also now considered to be the result of remobilized sands. Potentially, known fields such as Balder, with its steep sided reservoir, may also be re-categorized as an injectite rather than a deep marine fan reservoir. Utilizing a depth migrated seismic dataset with reduced artefacts from shallow anomalies may validate this and enable additional fields to be discovered.

Challenges to the seismic imaging include the relatively shallow (100 m) water depth and the geologically complex

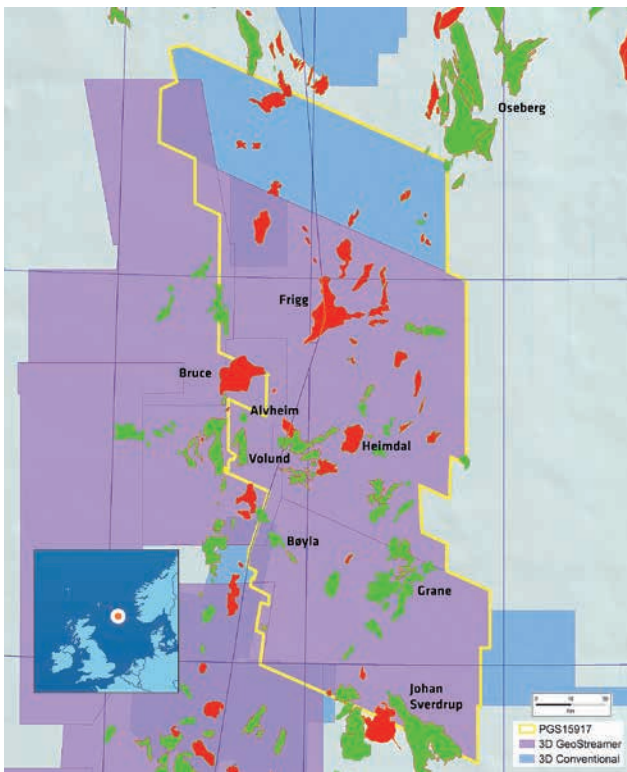


**Figure 1** Location of the Viking Graben multi-client PSDM survey (yellow outline) combining a number of early dual-sensor surveys into a single seamless depth volume. The new merged PSDM survey includes data acquired in JV partnership with TGS.

<sup>1</sup> PGS.

\* Corresponding author, E-mail: grunde.ronholt@pgs.com

## Data Processing

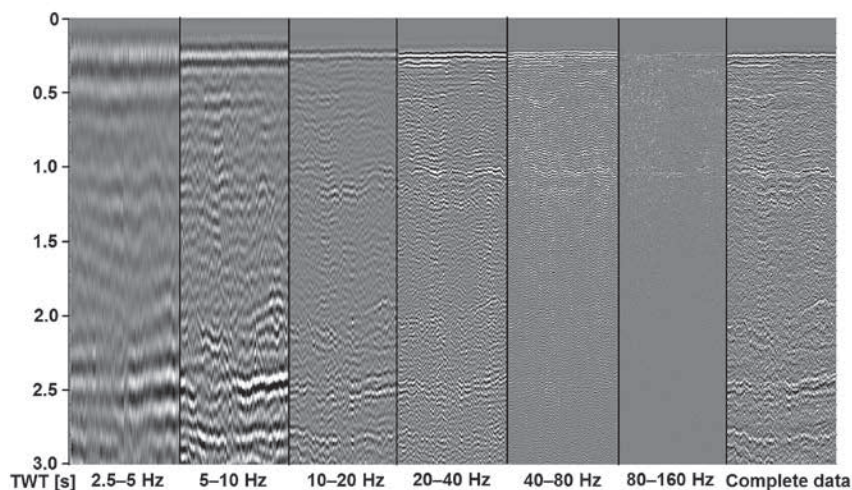


*Figure 2* Filter panels of the merged dual-sensor data after application of designation and source and receiver deghosting, illustrating the substantial energy recorded in the low to ultra-low part of the frequency spectrum.

near-surface section, which includes the widespread presence of channels of varying scales. Historically, these channels have had a profound impact on the seismic image quality at greater depth when not sufficiently characterized and accounted for during pre-stack migration. Dimming, pull-up and push-down effects have often created artificial geometries at various target levels, including around the Balder formation, the Base Cretaceous Unconformity (BCU) and even at deeper Jurassic levels.

Recognizing the potential for significant image improvements by applying the latest in enhanced signal processing, velocity model building and depth domain migration technology, a large-scale reprocessing project was initiated in 2016 combining the aforementioned dual-sensor surveys into a single 11,000 km<sup>2</sup> multi-client survey. In addition to ensuring accurate amplitude and phase treatment during source-side deghosting and designation, and the optimal removal of surface related multiples, a specific focus was placed on the creation of a detailed velocity model that included all shallow overburden features such as channels and sand injectites.

### Maximizing the signal bandwidth

To ensure the broadest possible signal bandwidth and to create a simple and robust seismic wavelet a careful source designation process was applied to all surveys. This process aims to address two different effects on the wavelet. Firstly, it addresses the amplitude and phase distortions caused by the source array signature, and secondly it corrects for the source ghost effect. Phase-only source de-ghosting is applied in the frequency-wavenumber domain to correctly account for the varying take-off angles. Amplitude corrections are applied at a later stage to avoid over-boosting of low frequency noise.

A designation filter was then designed and applied to zero phase the source wavelet and the system response and to remove the bubble effect. The source wavelet and

full system response is provided by the ghost free far-field signature. The low-frequency part of the far-field signature is derived from near-field hydrophone data, which provide a more accurate description of the bubble oscillation. The far-field signature is then shaped to a desired output spectrum derived from the full system response. The output wavelet itself is designed such that the total energy of the far-field signature is preserved and the side lobes are minimized.

This source designation process was separately applied to the different surveys prior to merging them into a single data volume. The stability of the amplitude and phase information across all frequencies was validated to ensure no additional statistical matching was required.

Figure 2 displays crossline frequency panels for the merged dataset, validating that designation and deghosting processes have ensured the preservation of substantial signal energy in the low to ultra-low frequency range.

### Removing multiples in a shallow water environment

One of the main challenges in processing shallow water seismic data is the successful removal of prominent surface related multiple energy that is generated by the seabed and other very shallow reflectors. In most cases the nearest receiver offsets are significantly larger than the water depth and little or no primary reflection energy is recorded. To enable the generation of a shallow overburden image around the water bottom, a prerequisite for data-driven multiple removal methods such as 3D SRME, model-based methods have been developed (Oukili et al., 2015).

The cascaded multiple attenuation flow applied to the regional reprocessing project described here comprised of two main steps. Firstly, two passes of multiple modelling by wavefield extrapolation combined with simultaneous adaptive subtraction were applied to address the short-period multiples. This was followed by a single pass of muted

convolutional 3D SRME to remove the remaining long-period multiples.

For the wavefield extrapolation modelling a one-way wave equation scheme was used to generate a surface-related multiple model. This was achieved by adding an additional round trip of the recorded data through the earth. This requires two auxiliary datasets: a cube that represents the earth's reflectivity and a corresponding 3D velocity field (Brittan et al., 2011).

For the first pass the required reflectivity cube was generated using synthetic water-bottom reflections whose two-way times were extracted from a near trace autocorrelation cube. For the second pass the reflectivity cube was generated by Separated Wavefield Imaging (PGS SWIM).

SWIM is an innovative depth imaging technology that uses both up-going and down-going wavefields, recorded by the co-located hydrophone and motion sensors in the dual-sensor streamer system (Whitmore et al., 2010). It effectively creates virtual sources at every receiver location in a marine seismic streamer spread which significantly enhances subsurface illumination and produces images of the seabed and shallow reflectors that primary reflections alone are not capable of (Figure 3).

Targeting of long-period multiples used a single pass of convolutional 3D SRME with a top mute set to coincide with the maximum depth used in the SWIM reflectivity cube. This effectively prevents the re-introduction of short-period multiples which were previously removed during the wavefield extrapolation demultiple step.

### Detailed velocity model building

As outlined by Rønholt et al. (2014), the key to producing a detailed velocity model that describes the complex overburden geology accurately lies in the way different algorithms are combined into a single velocity model building and imaging workflow. Specifically suited for shallow-water environments, the Complete Wavefield Imaging (CWI) processing workflow was consequently developed. This combines reflection tomography, full waveform inversion (FWI) and SWIM (see Figure 4).

The starting point of this workflow is the generation of an initial velocity model using sonic log information including well-derived anisotropic estimates. Optionally, a first pass of wavelet shift tomography can be run to ensure a globally consistent velocity field as input to FWI to avoid cycle skipping (Rønholt et al., 2014). FWI was performed over the total survey area which provided very detailed velocity updates down to a depth of 1 km. FWI results were selectively quality controlled using SWIM image gathers. For the deeper sections, reflection tomography was used with wavelet attributes generated by beam migration. In addition, targeted velocity inclusion followed by high resolution tomography was performed to introduce local velocity variation of geobodies (cemented sand bodies and injectites).

### Full waveform inversion

A novel gradient-based FWI algorithm was employed for this study which uses both reflected and transmitted wave modes. This is achieved by introducing dynamic weights in the velocity sensitivity kernel derived from impedance and velocity parameterization of the classical objective function. The new kernel implementation effectively eliminates the migration isochrones produced by the specular reflections and enhances the low wavenumber components in the gradient in heterogeneous media (Ramos-Martinez et al., 2016). This new FWI implementation reduces the traditional dependency on recording ultra-long offset information to achieve a velocity update at a greater burial depth.

The velocities of the main shallow channel features, with widths exceeding 1.5 km (Figure 5), were added to the model by interpretation, as they were not appropriately represented in the initial starting model. Including the channel features in the model resulted in a better match between modelled and recorded shots, enabling rapid convergence of the FWI updates across the regional dataset, and avoided any problems with cycle skipping.

FWI was performed using three increasingly larger frequency ranges from 2 Hz to 12 Hz. The FWI process successfully exploited the naturally rich low frequency

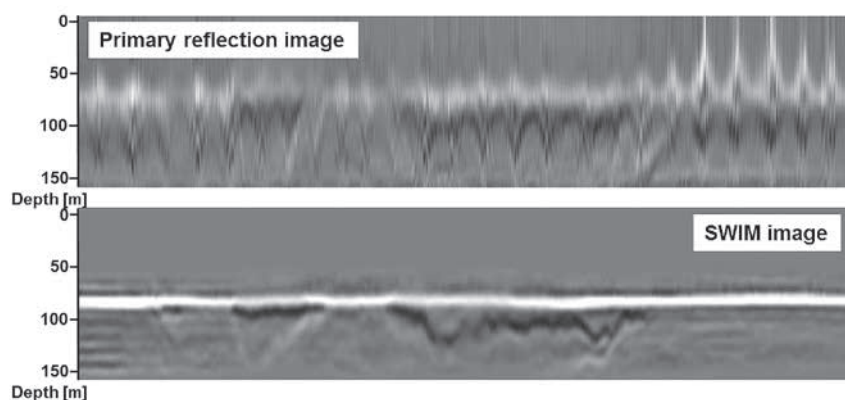


Figure 3 Crossline stacks from a near-offset primary reflection stack (top) and from the SWIM image (bottom), which was used as the near-surface reflectivity input for wave equation demultiple.

Data Processing

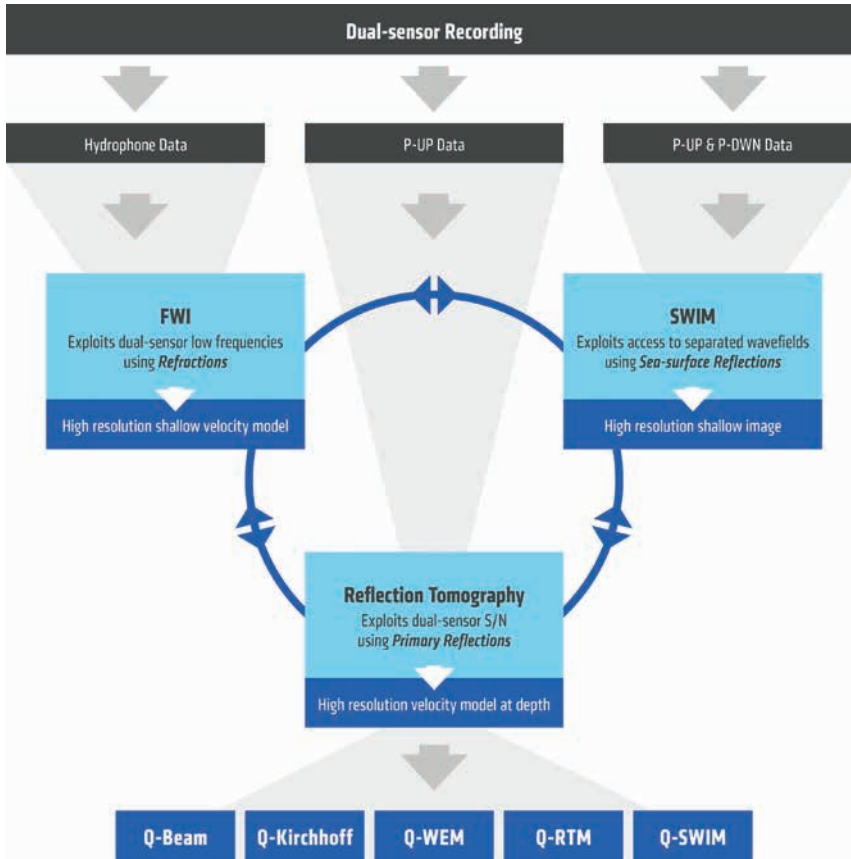
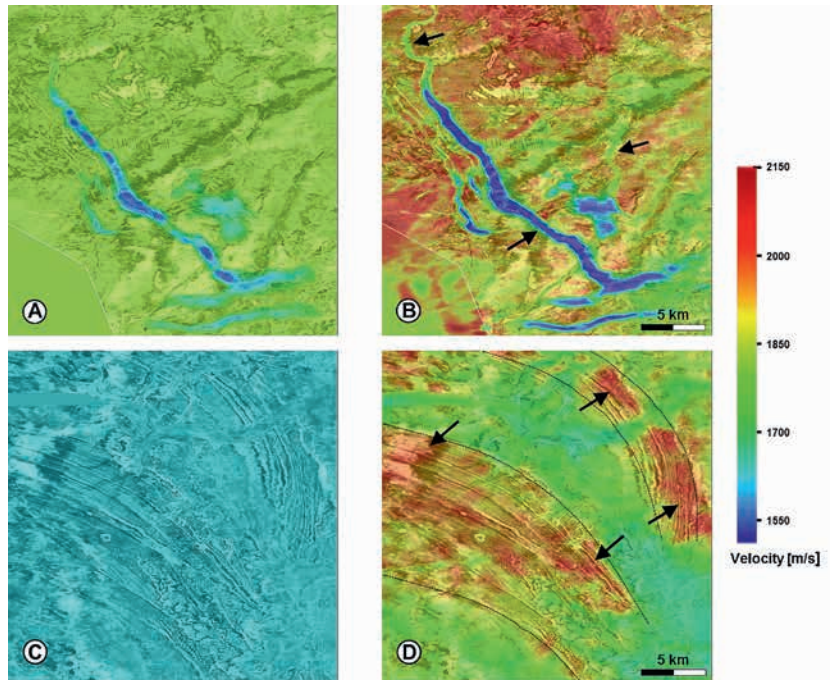


Figure 4 Complete Wavefield Imaging (CWI) workflow which leverages up-going and down-going wavefields that are generated as part of the dual-sensor receiver deghosting process.

Figure 5 Depth slices at depths of 195 m (upper panel) 415 m (lower panel) of the velocity depth model after FWI with the corresponding Kirchhoff depth migrated image overlaid. Section A and C represent the results for the initial velocity model, whereas section B and D show the results after FWI velocity estimation. Various geological features such as shallow channels (B) and clinoforms (D) can be identified in the updated velocity field.



content of dual-sensor data. The final velocity model was validated using a suite of beam migrations and on a set of SWIM image gathers, both of which demonstrated the

improvements in image quality, with most of the pull-up and push-down effects associated with the channel features being successfully corrected for.

Figure 5 shows a comparison of the PSDM velocity model before and after the FWI update. The final seismic image overlain with the respective velocity field is presented for two different depth positions. The upper panel of Figure 5 shows a horizontal slice through the final migrated image at 195 m depth and the associated initial velocity field (left) and the final FWI update (right). The FWI velocity attributes are characterized by significantly more detail and lateral variability, which correlates closely with structural features such as the paleo channels visible on the seismic (see arrows). The lower panel shows the same velocity improvements for a deeper depth slice at 415 m. Again, high and low velocities closely follow structural boundaries, demonstrating that the FWI inversion has successfully delineated features such as prograding clinoforms (bounded by dotted lines), which are now properly accounted for in the PSDM velocity model.

### Tomographic velocity estimation

Below the depth of approximately 1000 m the velocity update was continued with wavelet shift tomography over the 11,000 km<sup>2</sup> survey area. This specific tomographic solution was selected as it allowed for very rapid update cycles. In contrast to traditional tomographic approaches where a new set of residual move-out information picked on image gathers is used for each iteration, the tomographic approach used here utilizes the same wavelet attributes computed using a pre-stack beam migration formulation (Sherwood et al., 2008) for a number of iterations. 3D residuals after migration through a given velocity model are tomographically back-projected as slowness updates to the initial model (Sherwood et al., 2011). Initially, a couple of tomographic iterations were performed over the complete depth range below 1000 m before the model was divided up into 5 horizon bound units, confined by the Top

Balder, the Base Tertiary, the BCU and the Top Sleipner horizons. For each such stratigraphic unit, well-log derived sonic velocity trends were used to build the initial velocity field.

### Incorporating V-brights

Remobilized and injected sand bodies, also known as V-brights, often stand out in the seismic images as bright amplitude events, and frequently represent high-velocity anomalies that might cause unwanted pull-up effects and poor focusing when not accounted for in the velocity field used during migration. As they are relatively small in scale they were mechanically inserted as geobodies in the velocity model above the Balder level. Detection of the V-brights was achieved by automatically identifying the contrast of their high amplitudes against the background amplitude of the Grid formation. Once areas of locally high amplitude were identified, they were isolated into geobodies and a scalar was applied to the velocity field within those bodies. A local velocity increase of 20% has proven to be a pragmatic starting value. Finally, to allow for a small correction to velocity, high resolution tomography was performed, limiting the velocity updates to the geobodies only.

Figure 6 shows the final model above the Balder formation after successful FWI and tomographic velocity updates. The high velocity V-brights are clearly visible as are various other very detailed features such as shallow channels and prograding clinoforms.

Below Balder the tomographic update was continued in a top-down layer stripping fashion. A mis-ties analysis was performed for every key horizon as the velocity update proceeded and anisotropy parameters were adjusted to achieve a vertical positioning error of less than 1% between available well markers and the respective formation tops.

### Correcting for attenuation

Attenuation of seismic waves causes the loss of high-frequency energy and a general distortion of the phase of the seismic signal. Traditionally, an attenuation model is described by the quality factor, Q. Amplitude and phase distortions caused by attenuation and dispersion are best corrected for during pre-stack migration as it correctly accounts for the actual ray paths of the reflected signals and thus honours the 3D nature of the wavefield propagation (Valenciano and Chemingui, 2012).

Zhou et al. (2014) have demonstrated that detailed velocity information from FWI can be used to extract the geometry of gas clouds with high precision. Assuming a correlation between low velocity and low Q (high absorption), Zhou et al., successfully constrained their Q-tomography updates in the gas cloud locations.

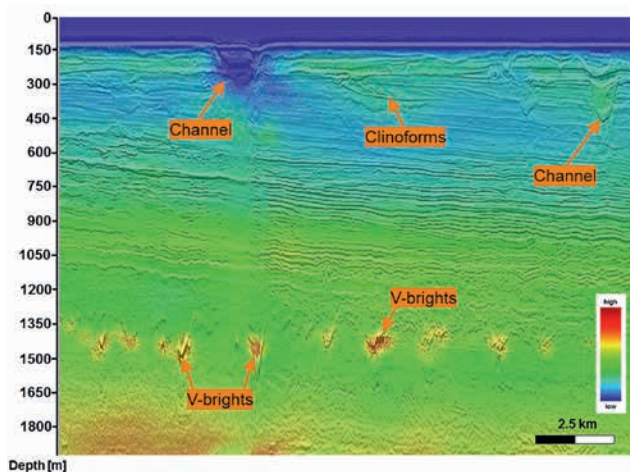
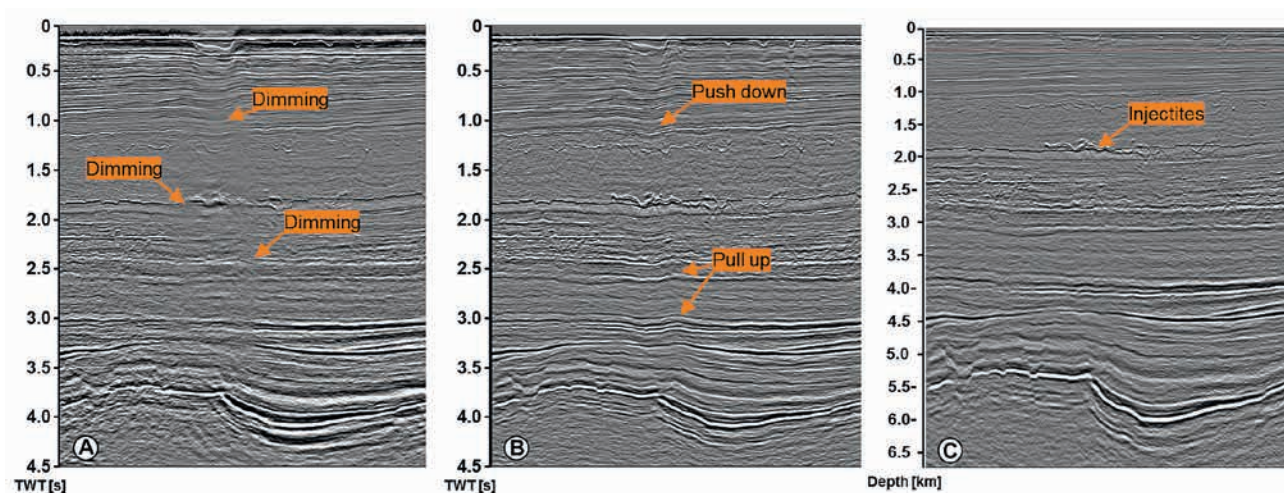
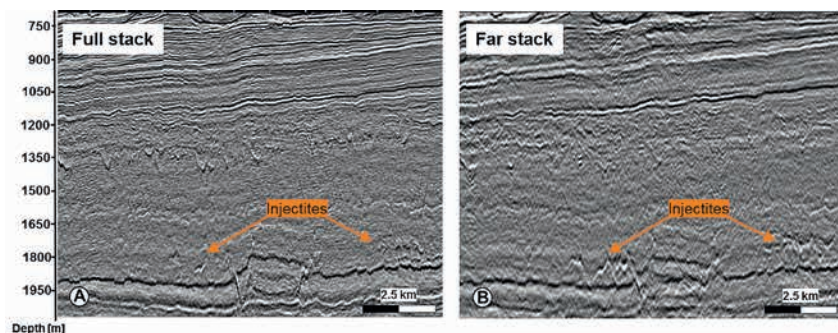


Figure 6 Final model above Balder after successful FWI and tomographic velocity updates, showing excellent correlation between structural features such as channels and injectites/clinoforms.

# Data Processing



**Figure 7** A) Pre-stack time migration image using the initial velocity model. B) Pre-stack depth migration result stretched to time using the final velocity model including attenuation compensation (Q). C) Pre-stack depth migration image using the final velocity and Q model. The updated velocity model produces a better focused image in the time domain (B) and push-down and pull-up artefacts are successfully corrected for in the final depth domain image (C).



**Figure 8** Comparison of full (0-40 degrees) and far angle (35-50 degrees) stacks. The significant far-off-set amplitude brightening of the injectites could be representative of Class 3 AVO behaviour and indicate the possible presence of hydrocarbon charge.

Here we have followed a similar approach by assuming that low velocity shallow channels are associated with low Q (high absorption). As can be seen from Figure 7A, there is indeed significant absorption in the shallow overburden beneath the main channel bodies, resulting in local dimming of amplitudes. Using the FWI and tomography velocity model only, we were able to build a spatially varying Q field as input to the depth migration.

By combining detailed velocity analysis with a structurally consistent Q-model for visco-acoustic depth migration, we have significantly reduced undesired imaging artefacts (Figure 7A and 7B), and achieved laterally consistent and reliable amplitude behaviour throughout the survey area (Figure 7C).

## Conclusions

This reprocessed multi-client data volume over the Viking Graben demonstrates how the combination of true broadband dual-sensor acquisition and advanced processing techniques can result in significantly improved image quality, which in turn increases the confidence in newly identified prospectivity within this mature basin.

Improvements in overall image quality were achieved by ensuring consistent amplitude and phase control during the

designature and deghosting processes with a specific focus on low frequencies, and by applying Q-compensation in the migration using a 3D Q model.

Building a detailed and geologically consistent migration model by utilizing different seismic wavefield components (reflections, refractions and multiples), uniquely available through dual-sensor data, for FWI and reflection tomography velocity updates proved critical for minimizing any pull-up and push-down effects in the final depth image. Additionally, amplitude dimming resulting from attenuation, as historically observed beneath some of the main shallow channels, has been successfully corrected for enabling confident pre-stack AVO extraction of potentially prospective remobilized sand bodies (Figure 8).

Significant hydrocarbon potential remains within the classic plays of the Viking Graben. The improvements in the structural imaging both in the shallower overburden and at depth achieved with this new dataset, coupled with unmatched AVO fidelity of the underlying dual-sensor data, could provide the necessary fresh input to trigger additional discoveries. The reduction in image degradation beneath the shallow anomalies has already enabled new targets in the shallower Tertiary sections to be identified. Several interesting geometries and seismic anomalies have been suc-

cessfully characterized within the Paleocene near the Volund and Heimdal fields, and initial investigations suggest good control of lithological and fluid delineation at these depths.

Although an intensely explored area of the Central North Sea the Viking Graben has certainly not revealed all its hydrocarbon secrets.

**Acknowledgements**

The authors would like to thank PGS for permission to publish this article. We also acknowledge TGS as our JV partner for a number of surveys included in this reprocessing project, and Det Norske Oljeselskap for valuable input.

**References**

Brittan, J., Martin, T., Bekara, M. and Koch, K. [2011] 3D shallow water demultiple – Extending the concept. *First Break*, 29, 97–101.

Oukili, J., Jokisch, T., Pankov, A., Farmani, B., Ronholt, G., Korsmo, Ø., Raya, P.Y. and Midttun, M. [2015] A novel 3D demultiple workflow for shallow water environments – a case study from the Brage field, North Sea. *77<sup>th</sup> EAGE Conference and Exhibition*, Expanded Abstracts, N114.

Ramos-Martinez, J., Crawley, S., Zou, Z., Valenciano, A.A., Qui, L. and Chemingui, N. [2016] A Robust Gradient for Long Wavelength

FWI Updates. *78<sup>th</sup> EAGE Conference and Exhibition*, Expanded Abstracts, SRS2.

Ronholt, G., Korsmo, Ø., Brown, S., Valenciano, A., Whitmore, D., Chemingui, N., Brandsberg-Dahl, S., Dirks, V. and Lie, J.-E. [2014] High-fidelity complete wavefield velocity model building and imaging in shallow water environments – A North Sea case study. *First Break*, 32, 127-131.

Sherwood, J., Sherwood, K., Tieman, H. and Schleicher, K. [2008] 3D beam pre-stack depth migration with examples from around the world. *78<sup>th</sup> SEG Annual Meeting*, Expanded Abstracts, 438–442.

Sherwood, J., Jiao, J., Tieman, H., Sherwood, K., Zhou, C., Lin, S. and Brandsberg-Dahl, S. [2011] Hybrid tomography based on beam migration. *81<sup>st</sup> SEG Annual Meeting*, Expanded Abstracts, 3979–3983.

Valenciano, A.A. and Chemingui, N. [2012] Viscoacoustic imaging: tomographic Q estimation and migration compensation. *82<sup>nd</sup> SEG Annual Meeting*, Expanded Abstracts, 1-5.

Whitmore, N.D., Valenciano, A.A., Söllner, W. and Lu, S. [2010] Imaging of primaries and multiples using a dual-sensor towed streamer. *80<sup>th</sup> SEG Annual Meeting*, Expanded Abstracts, 3187–3192.

Zhou, J., Wu, X., Teng, K., Xie, Y., Lefevre, F., Anstey, I. and Sirgue, L. [2014] FWI-guided Q Tomography for Imaging in the Presence of Complex Gas Clouds. *76th EAGE Conference and Exhibition*, Expanded Abstracts, E106.

**Caen - France**  
**RST 2016**  
**24-28**  
**October 2016**

**EARTH SCIENCES MEETING**  
 25<sup>th</sup> EDITION

[www.rst-sgf.fr](http://www.rst-sgf.fr)

**Job Prospects & Education Forum**

12 main themes    Plenary lectures    Field trips    Exhibition space

SGF    UNICAEEN    Normandie Université    UNIVERSITÉ DE ROUEN    CNRS

© BRGM-RL Coefflé (vue sur le Cap de la Percée depuis la plage d'Omaha Beach, falaise calcaire du Bathonien)